Individual Reduction Potentials of the Iron Ions in Fe_2S_2 and High-Potential Fe_4S_4 Ferredoxins

Lucia Banci,[†] Ivano Bertini,*[,†] Giovanni Gori Savellini,[†] and Claudio Luchinat[‡]

Department of Chemistry, University of Florence, Florence, Italy, and Institute of Agricultural Chemistry, University of Bologna, Bologna, Italy

Received January 17, 1996[⊗]

The DelPhi program package has been used to confirm that the span in reduction potentials among high-potential Fe_4S_4 ferredoxins must be mainly ascribed to the net protein charges arising from acidic and basic residues. Subsequently, the order of the individual reduction potentials of the iron ions in Fe_2S_2 ferredoxins as found from NMR spectroscopy was explained mainly on the basis of different solvation contributions to the electrostatic potential. The individual reduction potentials of the iron ions in high-potential Fe_4S_4 ferredoxins, again available from NMR spectroscopy, are only qualitatively reproduced. It is proposed that the protein triggers a distortion in the cluster which would be a further contribution to the electrochemical inequivalence of the individual iron ions.

Introduction

Understanding the factors determining the reduction potentials of proteins involved in electron-transfer processes has long interested biophysical scientists.[1−7] Essentially, the electrostatic contributions to the reduction potentials can be classified as arising from (a) the fractional charges of the protein atoms, (b) the protein charges induced by polarization mechanisms, (c) the net charges of ionizable residues, and (d) solvation effects.

The Fe_4S_4 center in high-potential ferredoxins (abbreviated HiPIP from high-potential iron−sulfur protein) and low-potential ferredoxins (or simply ferredoxins), which undergoes one-electron redox processes, spans quite different redox states: HiPIPs involve a $[Fe_4S_4]^{3+/2+}$ redox pair, whereas ferredoxins involve a $[Fe_4S_4]^{2+/1+}$ pair. The redox potentials of these proteins may differ by as much as 1 V.[1] This striking difference has been largely explained on the basis of the different dipolar electric fields produced by the peptide bonds around the polymetallic center.[8] On the other hand, the redox potential range from 90 to 450 mV observed in HiPIPs[9] has been explained mainly on the basis of the different electrostatic effects due to net charges of ionized residues.[10] This contrasts with what has been observed for a series of cytochromes, where no relation between the overall net charge and the reduction potential exists within the series.[11] On the other hand, local charge effects are observed in tetraheme cytochromes, where the interactions between the reaction centers and specific ionized sites were shown to be the main factor influencing the individual midpoint potential of each of the four hemes.[12]

A major problem in the analysis of the electrostatic interactions is the discontinuity between the water medium and the protein medium.[13−16] The partial charges of the water and protein atoms are rather reliable and are able to account for many macroscopic properties.[17−20] These charges are believed to provide good estimates of the internal energy term for electrostatic interactions. However, solvation contributions can only be treated properly, in microscopic models, with full free energy calculations. The latter calculations are extremely demanding and represent a drawback when the description of reduction potentials of redox proteins is attempted. Furthermore, the charges of open-shell metal ions and their donor atoms are more difficult to evaluate than those of protein atoms.[6,21] Recently, density functional approaches seem to have permitted reasonable estimates of charges in iron−sulfur clusters.[22]

Warshel et al. decompose the protein part into dipoles, and the water molecules are approximated by Langevin dipoles.[16]

* Corresponding author. Phone: +39-55-2757549. Fax: +39-55-2757555. E-mail: bertini@risc1.lrm.fi.cnr.it.
[†] University of Florence.
[‡] University of Bologna.
[⊗] Abstract published in *Advance ACS Abstracts,* June 1, 1996.

(1) Carter, C. W. J. *J. Biol. Chem.* **1977**, *252*, 7802−7811.
(2) Kassner, R. J.; Yang, W. *J. Am. Chem. Soc.* **1977**, *99*, 4351−4355.
(3) Sheridan, R. P.; Allen, L. C.; Carter, C. W. J. *J. Biol. Chem.* **1981**, *256*, 5052−5057.
(4) Rogers, N. K.; Moore, G. R.; Sternberg, M. J. E. *J. Mol. Biol.* **1985**, *182*, 613−616.
(5) Markley, J. L.; Chan, T. M.; Krishnamoorthi, R.; Ulrich, E. L. *Iron-Sulfur Research*; Springer-Verlag: New York, 1987; pp 167−184.
(6) Davis, M. E.; McCammon, J. A. *Chem. Rev.* **1990**, *90*, 509−521.
(7) Shen, B.; Jollie, D. R.; Stout, C. D.; Diller, R. C.; Armstrong, F. A.; Gorst, C. M.; La Mar, G. N.; Stephens, P. J.; Burgess, K. *J. Biol. Chem.* **1994**, *269*, 8564−8575.
(8) Jensen, G. M.; Warshel, A.; Stephen, P. J. *Biochemistry* **1994**, *33*, 10911−10924.
(9) Luchinat, C.; Capozzi, F.; Borsari, M.; Battistuzzi, G.; Sola, M. *Biochem. Biophys. Res. Commun.* **1994**, *203*, 436−442.
(10) Banci, L.; Bertini, I.; Ciurli, S.; Luchinat, C.; Pierattelli, R. *Inorg. Chim. Acta* **1995**, *240*, 251−256.
(11) Moore, G. R.; Pettigrew, G. W. *Cytochromes c: Evolutionary, Structural and Physicochemical Aspects*; Springer-Verlag: Berlin, 1990.
(12) Gunner, M. R.; Honig, B. *Proc. Natl. Acad. Sci. U.S.A.* **1991**, *88*, 9151−9155.
(13) McCammon, J. A.; Harvey, S. C. *Dynamics of proteins and nucleic acids*; Cambridge University Press: Cambridge, U.K., 1987.
(14) Knapp, E. W.; Muegge, I. *J. Phys. Chem.* **1993**, *97*, 11339−11343.
(15) Harvey, S. C. *Proteins: Struct., Funct., Genet.* **1989**, *5*, 78−92.
(16) Warshel, A.; Russell, S. T. *Q. Rev. Biophys.* **1984**, *17*, 283−422.
(17) Cornell, W. D.; Cieplak, P.; Bayly, C. I.; Gould, I. R.; Merz, K. M.; Ferguson, D. M.; Spellmeyer, D. C.; Fox, T.; Caldwell, J. W.; Kollman, P. A. *J. Am. Chem. Soc.* **1995**, *117*, 5179−5197.
(18) Tannor, D. J.; Marten, B.; Murphy, R.; Friesner, R. A.; Sitkoff, D.; Nicholls, A.; Ringnalda, M.; Goddard, W. A., III; Honig, B. *J. Am. Chem. Soc.* **1996**, *116*, 11875−11882.
(19) Brooks, C. L, III; Karplus, M.; Petitt, B. M. *Proteins: a perspective of dynamics, structure and thermodynamics*; J. Wiley and Sons: New York, 1988.
(20) Jorgensen, W. L.; Chandrasekhar, J.; Madura, J.; Impey, R. W.; Klein, M. L. *J. Chem. Phys.* **1983**, *79*, 926−935.
(21) Comba, P.; Hambley, T. W. *Molecular Modeling of Inorganic Compounds*; VCH: Weinheim, Germany, 1995.
(22) Mouesca, J. M.; Chen, J. L.; Noodleman, L.; Bashford, D.; Case, D. A. *J. Am. Chem. Soc.* **1994**, *116*, 11898−11914.

S0020-1669(96)00051-1 CCC: $12.00

The protein and its shell of Langevin dipoles are immersed in a continuum medium representing bulk water. Purely continuum models are also available.[18,23−25] A program called DelPhi, proposed by Honig et al.,[26] is based on the solution of the classical Poisson−Boltzmann equation to describe any charge distribution in the system. Water and protein constitute two continuum media characterized by two different dielectric constants.

Some of our group had used the AMBER program package[27] to equilibrate the protein and water molecules and computed the electrostatic potentials of the polymetallic centers by using the partial charges and induced charges, in a medium with average dielectric constant.[10] In this paper, we use the DelPhi program[26] to analyze the factors determining the reduction potentials in a series of high-potential ferredoxins to test the agreement with our previous treatment. The two treatments can be considered at the extremes of the range of possible theoretical approaches. The results for this series of proteins turn out to be essentially model-independent. Furthermore, we address here the problem of rationalizing the different reduction potentials of the individual iron ions both in the Fe_4S_4 center of HiPIPs and in a Fe_2S_2 center of a ferredoxin. The relative individual redox potentials are estimated from NMR measurements,[28,29] as will be discussed. Besides some weaknesses in the quantitative results, a satisfactory picture starts to emerge.

Materials and Methods

The X-ray structure coordinates of the algal Fe_2S_2 ferredoxin from *Spirulina platensis* (PDB file ID: 4fxc),[30] and of the Fe_4S_4 HiPIPs from *Ectothiorhodospira halophila* (iso-I) (2hip),[31] *Rhodocyclus tenue* (1isu),[32] *Chromatium vinosum*[33] (1hip), and *Ectothiorhodospira vacuolata* (iso-II) (1hpi)[34] were used as starting data. In the case of HiPIPs from *E. halophila* (iso-II), *E. vacuolata* (iso-I), and *Rhodocyclus gelatinosus*, for which X-ray structures are not available, previously obtained average molecular dynamics (MD) structures[10] were used. Both sets of structures were solvated with a 16 Å thick shell of water molecules. The water molecules were equilibrated by MD keeping the protein atoms fixed, and finally the whole systems (water + protein) were energy-minimized.[10] After this procedure, the structures derived from the X-ray coordinates have an rms deviation of 0.3−0.5 Å with respect to the starting crystallographic structures. The structures derived from MD models had been previously checked for folding homology with those for which X-ray structures were available.[10] In particular, the whole H-bonding network around the cluster is always strictly maintained. The electrostatic potential calculations were performed with the DelPhi program package which solves the Poisson−Boltzmann equation when a distribution of charges and dielectric constants is given.[35,36] A radius was assigned to all the protein atoms from the DelPhi database. The effect of varying dielectric constants (from 1 to 15) for the protein interior was analyzed (see Results and Discussion), while a dielectric constant of 80 was used for the solvent. A probe radius of 1.4 Å, which defines the water-accessible surface, was chosen. The partial charges of the protein atoms were taken from the AMBER "united-atom" database.[37] Density functional ESP point charges (DFT-ESP)[22] were used for the $[Fe_2S_2]^{2+/1+}$ cluster of Fe_2S_2 ferredoxin and for the $[Fe_4S_4]^{2+/3+}$ cluster in HiPIPs. The AMBER partial charges of cysteine ligands were modified by assigning DFT-ESP charges[22] to the S and Cβ atoms and by redistributing the difference between the DFT-ESP charges and AMBER charges over the Hβ and Cα cysteine atoms in such a way as to preserve the total charge of the residue. Then the protein structures were mapped onto a $65 \times 65 \times 65$ point grid and the Poisson−Boltzmann equation was iteratively solved using a finite difference method.[36,38] To ensure that the calculations were not sensitive to grid dimensions, a series of three focusing calculations were performed.[26] The final grid spacing was 1.5 grids/Å. The electrostatic free energy of reduction (ΔG_{red}) is the sum of the following terms: (1) pairwise interactions of the iron cluster charges with the protein charges, screened by the polarizability of the protein and the solvent ($\Delta G_{ch} + \Delta G_{dip}$);[39] (2) the reaction field energy (solvation energy) due to the polarization of electrons and dipoles in the solvent and protein induced by the reduction of the Fe_2S_2/Fe_4S_4 cluster ($\Delta\Delta G_{solv}$).[40] The contribution of the protein charges has been further factorized into the two terms previously mentioned: ΔG_{ch} is the contribution due to the net charges of the protein, and ΔG_{dip} is the contribution due to the protein dipoles produced by all the partial charges on all protein atoms but those of the charged residues. ΔG_{ch} was evaluated by assigning the AMBER charges to the charged residues (Asp, Glu, Arg, and Lys) and null charges to the rest of the protein. The contribution to ΔG_{dip} due to the H-bonds and dipoles derived from CONH peptide groups (ΔG_{CONH}) was evaluated as the difference between a calculation of ΔG_{dip} as described above and the same calculation performed not including the charges on the CONH atoms. The latter calculation was performed by assigning each of the four atoms one-fourth of the total charge of the CONH group, which amounts to −0.062. This ensures that the overall charge of the protein is not altered.

Results and Discussion

1. Macroscopic Reduction Potentials. The reduction potentials as calculated with the DelPhi program for the seven Fe_4S_4 HiPIPs are shown in Figure 1 for a water dielectric constant of 80 and a protein dielectric constant between 4 and 15, respectively. It should be noted that the calculated order of the reduction potentials reasonably follows the experimental one (with one exception). An overall satisfactory quantitative agreement is obtained with a protein dielectric constant of 15. However, this value is considered unrealistically large.[12,14,15,18] The value of the protein dielectric constant has been measured in the range 2−4.[41,42] These values can be used in electrostatic calculations if the distribution of charges is correctly estimated (i.e., if it could correctly reproduce electronic and reorientational polarization effects)[6,15] and if the electrostatic behavior of water is exactly reproduced. Previously, an average dielectric constant of 60 for this protein−water system was proposed.[10] Values for the dielectric constant larger than 4 have frequently been

(23) Sharp, K.; Honig, B. *Annu. Rev. Biophys. Biophys. Chem.* **1990**, *19*, 301−332.
(24) Gilson, M. K.; Honig, B. *Nature* **1987**, *330*, 84.
(25) Davis., M. E.; McCammon, J. A. *Chem. Rev.* **1990**, *90*, 509−521.
(26) Gilson, M. K.; Sharp, K. A.; Honig, B. H. *J. Comput. Chem.* **1988**, *9*, 327−335.
(27) Pearlman, D. A.; Case, D. A.; Caldwell, G. C.; Siebel, G. L.; Singh, U. C.; Weiner, P.; Kollman, P. A. *AMBER 4.0;* University of California: San Francisco, 1991.
(28) Babini, E.; Bertini, I.; Borsari, M.; Capozzi, F.; Dikiy, A.; Eltis, L. D.; Luchinat, C. *J. Am. Chem. Soc.* **1996**, *118*, 75−80.
(29) Bertini, I.; Ciurli, S.; Luchinat, C. *Structure and Bonding*; Springer-Verlag: Berlin, Heidelberg, 1995; Vol. 83, pp 1−54.
(30) Tsukihara, T.; Fukuyama, K.; Nakamura, M.; Katsube, Y.; Tanaka, N.; Kakudo, M.; Wasa, K.; Hase, T.; Matsubara, H. *J. Biochem.* **1981**, *90*, 1763−1773.
(31) Breiter, D. R.; Meyer, T. E.; Rayment, I.; Holden, H. M. *J. Biol. Chem.* **1991**, *266*, 18660−18667.
(32) Rayment, I.; Wesemberg, G.; Meyer, T. E.; Cusanovich, M. A.; Holden, H. M. *J. Mol. Biol.* **1992**, *228*, 672.
(33) Carter, C. W. J.; Kraut, J.; Freer, S. T.; Xuong, N.-H.; Alden, R. A.; Bartsch, R. G. *J. Biol. Chem.* **1974**, *249*, 4212−4215.
(34) Benning, M. M.; Meyer, T. E.; Rayment, I.; Holden, H. M. *Biochemistry* **1994**, *33*, 2476−2483.
(35) Gilson, M. K.; Rashin, A.; Fine, R.; Honig, B. *J. Mol. Biol.* **1985**, *183*, 503−516.
(36) Klapper, I.; Hagstrom, R.; Fine, R.; Sharp, K.; Honig, B. *Proteins: Struct., Funct., Genet.* **1986**, *1*, 47−59.
(37) Weiner, S. J.; Kollman, P. A.; Case, D. A.; Singh, U. C.; Ghio, C.; Alagona, G.; Profeta, S., Jr. *J. Am. Chem. Soc.* **1984**, *106*, 765−784.
(38) Warwicker, J.; Watson, H. C. *J. Mol. Biol.* **1982**, *157*, 671−682.
(39) Gilson, M. K.; Honig, B. *Proteins: Struct., Funct., Genet.* **1988**, *3*, 32−52.
(40) Gilson, M. K.; Honig, B. *Proteins: Struct., Funct., Genet.* **1988**, *4*, 7−18.
(41) Takashima, S.; Schwan, H. P. *J. Phys. Chem.* **1965**, *69*, 4176−4182.
(42) Pennock, B. D.; Schwan, H. P. *J. Phys. Chem.* **1969**, *73*, 2600−2610.

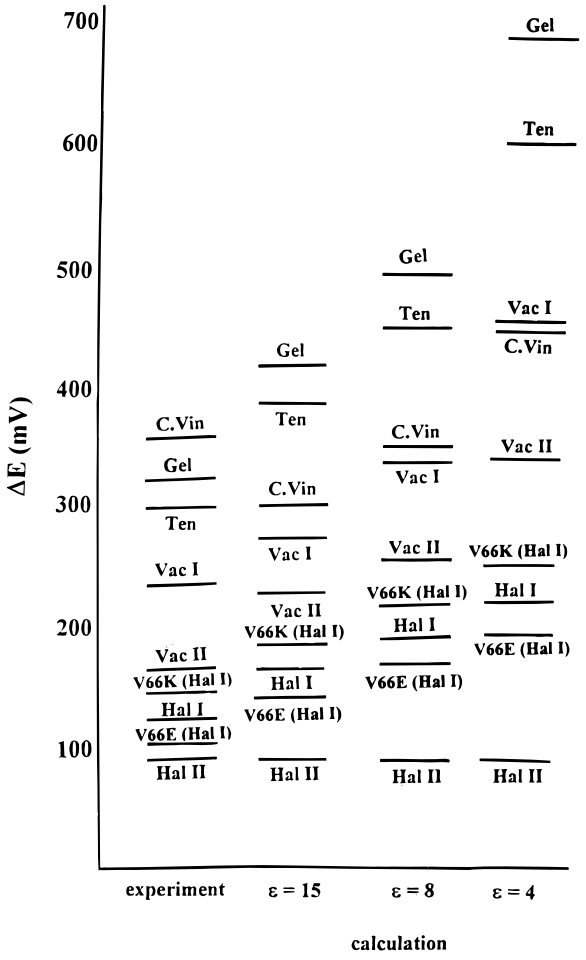

Figure 1. Experimental[9] (left column) and calculated reduction potentials of HiPIPs from *E. halophila* (iso I and II), *E. vacuolata* (iso I and II), *R. gelatinosa*, *C. vinosum*, and *R. tenue* for various values of the protein dielectric constant (right three columns).

used.[12,16,43−47] and found to be necessary to reproduce experimental data.[46,47] Also, from MD calculations, the estimate of the dielectric constant has led to relatively high values.[47] This point is the subject of a large debate in the literature;[14,15,18,46] the high values estimated for the dielectric constant have been proposed to be due to the large fluctuations of the protein dipole moment as a consequence, essentially, of the mobility of side-chain atoms (especially of ionized side-chain atoms).[46,47] It has been also suggested that the use of high values for the protein dielectric constant could take into account the omission of the effects produced by local conformational changes and specific ion binding.[46] Finally, it is possible that an incorrect distribution of charges on the iron ions and their ligands causes an error in the evaluation of the electrostatic interactions in the vicinity of the polymetallic center. However, sample calculations with grossly altered charge distributions in the cluster (not shown) indicate that the latter source of error is relatively minor.

Besides the quantitative agreement, the factors determining the relative reduction potentials have been evaluated by computing the effect of the single contributions as described under Materials and Methods. The results are shown in Figure 2 and are in substantial agreement with the previous analysis based on a pure Coulombic model.[10] The effect of dipoles and solvation is constant along the series whereas the effect of the net charges is significant. This has been experimentally verified by following the pH dependence of the reduction potential due to the deprotonation of histidines in HiPIPs[9] and by replacing Val 68 with Glu or Lys residues in HiPIP I from *E. halophila*.[48] Calculations have been also performed on the last two mutants to check the validity of the model through the effect of the variation of a single charge. The results are in very good agreement with the experiments (see Figure 1): the reduction potential of the V68E mutant is calculated to decrease by 20−30 mV with respect to the wild type, depending on the ϵ value ($\Delta E_{exp} = -25$ mV), and that of the V68K mutant to increase by 20−30 mV ($\Delta E_{exp} = +20$ mV). We consider our previous AMBER calculations and the present calculations using DelPhi to represent two extreme approaches to the evaluation of reduction potentials in proteins. The first is totally microscopic, while the latter treats the system as a continuum. As the results obtained with the two methods for the present series of proteins are very similar, we believe that they can be considered substantially model-independent and that other methods using a combination of microscopic and continuum treatments would also yield similar results.

2. Individual Reduction Potentials. With confidence taken from the above results that the DelPhi program can be helpful in predicting the macroscopic redox behavior of Fe−S proteins, we tried to account for the reduction potentials of the individual iron ions in the same cluster. The latter should depend on the same factors analyzed above, although more fine effects are considered in this case.

The Fe_2S_2 Case. The reduced $[Fe_2S_2]^+$ ferredoxin contains a ferric iron antiferromagnetically coupled to a ferrous iron.[49] Mössbauer spectra clearly distinguish the two irons in different oxidation states.[50] The ^{1}H-NMR spectra at room temperature provide a set of signals assigned to βCH_2 protons of cysteines bound to Fe^{3+} and another set of signals assigned to βCH_2 protons of cysteines bound to Fe^{2+}.[51] The sequence-specific assignment of the cysteine protons has shown that the iron(II) is that bound to Cys 41 and Cys 46 (Fe_A hereafter):[52] this is the iron ion that undergoes reduction when one electron is added to the oxidized $[Fe_2S_2]^{2+}$ protein containing two iron(III) ions. Fe_A is the iron closer to the surface of the protein.[3] An analogous result was obtained on another Fe_2S_2-containing protein.[53,54] From the room-temperature NMR data a $\Delta\Delta E$ value larger than 30 mV could be estimated.[29]

It was soon noted[3] that different numbers of H-bonds are present in the domains of the two iron ions. Indeed, in the environment of the more reducible Fe_A ion, four H-bonds are present (NH of Ala 45 and NH of Ala 43 interact with the coordinated sulfur atom of Cys 41; NH of Thr 48 and OH of

(43) Matthew, J. B. *Annu. Rev. Biophys. Biophys. Chem.* **1985**, *14*, 387−417.
(44) Gilson, M. K.; Honig, B. H. *Biopolymers* **1986**, *25*, 2097−2119.
(45) Sternberg, M. J. E.; Hayes, F. R. F.; Russell, A. J.; Thomas, P. G.; Fersht, A. R. *Nature* **1987**, *330*, 86−88.
(46) Antosiewicz, J.; McCammon, J. A.; Gilson, M. K. *J. Mol. Biol.* **1994**, *238*, 415−436.
(47) Smith, P. E.; Brunne, R. M.; Mark, A. E.; van Gunsteren, W. F. *J. Phys. Chem.* **1996**, *97*, 2009−2014.
(48) Bertini, I.; Borsari, M.; Bosi, M.; Eltis, L. D.; Felli, I. C.; Luchinat, C.; Piccioli, M. *J.B.I.C.*, in press.
(49) Dunham, W. R.; Palmer, G.; Sands, R. H.; Bearden, A. J. *Biochim. Biophys. Acta* **1971**, *253*, 373−384.
(50) Dunham, W. R.; Bearden, A. J.; Salmeen, I.; Palmer, G.; Sands, R. H.; Orme-Johnson, W. H.; Beinert, H. *Biochim. Biophys. Acta* **1971**, *253*, 134−152.
(51) Bertini, I.; Lanini, G.; Luchinat, C. *Inorg. Chem.* **1984**, *23*, 2729−2730.
(52) Dugad, L. B.; La Mar, G. N.; Banci, L.; Bertini, I. *Biochemistry* **1990**, *29*, 2263−2271.
(53) Skjeldal, L.; Markley, J. L.; Coghlan, V. M.; Vickery, L. E. *Biochemistry* **1991**, *30*, 9078−9083.
(54) Skjeldal, L.; Westler, W. M.; Oh, B.-H.; Krezel, A. M.; Holden, H. M.; Jacobson, B. L.; Rayment, I.; Markley, J. L. *Biochemistry* **1991**, *30*, 7363−7368.

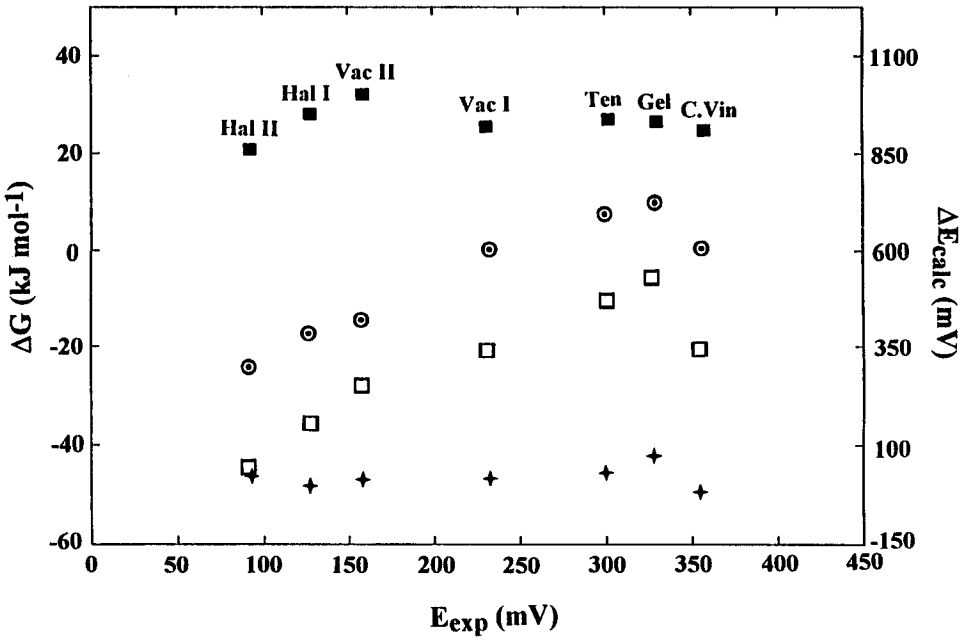

Figure 2. Plot of the calculated reduction potentials ($\epsilon_{protein} = 8$) (□) and of the contributions to the electrostatic energy from net charges (⊙), dipoles (■), and solvation (+) with respect to the experimental reduction potentials.

Table 1. Calculated Reduction Potentials and Variations in Free Energy between the Reduced and the Oxidized Form for the $[Fe_2S_2]^{2+/1+}$ Moiety in *S. platensis*[a]

	Fe_A	Fe_B	Δ_{AB}
$\Delta\Delta G_{solv}$[b]	75.5	82.8	−7.3
ΔG_{ch}[b]	21.6	22.5	−0.9
ΔG_{dip}[b]	−25.6	−24.4	−1.2
ΔG_{red}[b]	71.6	80.9	−9.3
ΔE[c]	−400	−497.1	97.1

[a] The values are calculated (with $\epsilon_{protein} = 4$) in the case of reduction of Fe_A or Fe_B (see text). [b] kJ mol^{-1}. [c] mV.

Ser 40 interact with the coordinated sulfur atom of Cys 46), while the environment of the other iron ion (Fe_B) is involved in only one H-bond (NH of Gly 44 interacts with the coordinated sulfur atom of Cys 79).[3] It is known that H-bonds provide positive fractional charges that can stabilize the extra negative charge added to the metal ion upon reduction. In Table 1 the results of the electrostatic potential calculations on Fe_2S_2 *S. platensis* ferredoxin performed with the DelPhi program are summarized. The calculations were performed by placing the extra electron alternatively more on the Fe_A or on the Fe_B site. According to the DFT-ESP charges,[22] the reduced iron site was assigned an excess charge of −0.235 with respect to the oxidized iron site. These calculations reproduce correctly the experimental data because they clearly identify Fe_A as the more reducible one. Indeed, the calculated redox potential difference is $\Delta\Delta E = 97.1$ mV (at pH = 7.0 and $T = 298$ K) for a dielectric constant of 4 and is inversely proportional to this parameter. Such $\Delta\Delta E$ values (ranging from 24 to 400 mV, depending on the dielectric constant) indicate that the valences are substantially localized. Even for a $\Delta\Delta E$ value of 24 mV corresponding to the high dielectric constant of 15, more than 70% localization of the extra electron on Fe_A is obtained.

We then analyzed the various factors contributing to ΔG_{red}, and therefore to $\Delta\Delta E$. They originate from the solvation energy (ΔG_{solv}) and from the electrostatic interactions of the cluster with the net charges of the protein (ΔG_{ch}) and with the protein dipoles (ΔG_{dip}). The latter term includes the contribution from the CONH dipoles (ΔG_{CONH}), which were also evaluated independently (see Materials and Methods for details of calculations). This analysis shows that all factors combine to stabilize the extra electron charge on Fe_A. The calculations show that solvation effects are the most important in stabilizing the reducible site, whereas fractional and net charges play a minor role. The variation of solvation energy of the cluster upon reduction, Δ_{AB}, differs by as much as −7.3 kJ mol^{-1}, depending on whether the extra electron is placed on Fe_A or Fe_B (Table 1). Among fractional charges, the stabilization of the reduced Fe_A center (contributing another −1.2 kJ mol^{-1}, Table 1) is essentially due to the positive end of the CONH dipoles pointing toward Fe_A (this effect includes H-bonds from peptide NH to iron donors). Net charges of acidic and basic residues contribute a further −0.9 kJ mol^{-1} (Table 1). In summary, we have shown that the same treatment capable of explaining the wide range of macroscopic reduction potentials within the series of HiPIPs is also able to account for the large experimental difference between the individual reduction potentials in Fe_2S_2 ferredoxins.

The Fe_4S_4 Case. As a further challenge, the individual reduction potential within the $[Fe_4S_4]^{3+}$ center in HiPIPs was calculated. Such a center contains one $Fe^{2.5+}$ mixed-valence pair and two Fe(III) ions,[29,55] while the $[Fe_4S_4]^{2+}$ cluster contains four equivalent $Fe^{2.5+}$ ions.[55,56] Electron delocalization over two of the four iron centers, as opposed to either fully localized or fully delocalized situations, is invariably observed experimentally[29] and is theoretically predicted to be the most stable from the electronic point of view.[57] In the oxidized form of these proteins, the mixed-valence pair could be located on each of the six edges of the Fe_4S_4 cube. It has been suggested that the protein component determines the valence distribution.[29,58] In HiPIP II from *E. halophila*, the mixed-valence pair is the one bound to Cys 42 and Cys 55, and only this distribution is present.[59] Other HiPIPs have a more complicated behavior with

(55) Middleton, P.; Dickson, D. P. E.; Johnson, C. E.; Rush, J. D. *Eur. J. Biochem.* **1980**, *104*, 289−296.
(56) Moss, T. H.; Bearden, A. J.; Bartsch, R. G.; Cusanovich, M. A. *Biochemistry* **1968**, *7*, 1591−1596.
(57) Bominaar, E. L.; Borshch, S. A.; Girerd, J.-J. *J. Am. Chem. Soc.* **1994**, *116*, 5362−5372.
(58) Banci, L.; Bertini, I.; Luchinat, C. *Struct. Bonding* **1990**, *72*, 113−135.

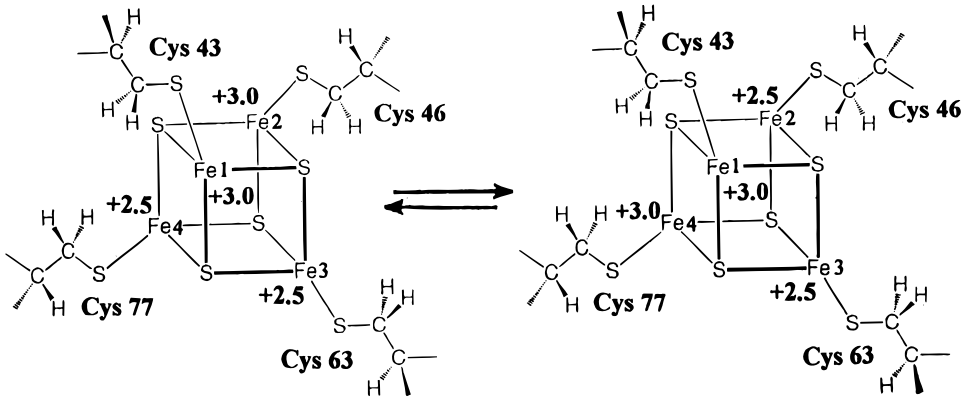

Figure 3. Scheme of the equilibrium between two valence distributions in the Fe_4S_4 cluster of the HiPIP from *C. vinosum*.

Table 2. Variations in Free Energy upon Reduction of the $[Fe_4S_4]^{3+/2+}$ Clusters in HiPIP II from *E. halophila* and in HiPIP from *C. vinosum* for Different Locations of the Mixed-Valence Pair in the Oxidized Form (Calculated with $\epsilon_{protein} = 1$)

E. halophila		*C. vinosum*	
mixed-valence pair	ΔE^a	mixed-valence pair	ΔE^a
Fe2−Fe3[b]	0.0	Fe3−Fe4[c]	0.0
Fe3−Fe4	−7.0	Fe2−Fe3[c]	0.0
Fe3−Fe1	−7.0	Fe2−Fe4	−2.0
Fe2−Fe4	−12.0	Fe1−Fe3	−5.0
Fe2−Fe1	−12.0	Fe1−Fe2	−8.0
Fe1−Fe4	−14.0	Fe1−Fe4	−8.0

[a] These values are referred to the more stable pair. Values are in mV. [b] Experimentally identified mixed-valence pair. [c] Experimentally identified mixed-valence pairs, approximately 60%:40% ratio in *C. vinosum*.

respect to the valence distribution.[60,61] This behavior has been investigated in detail by NMR techniques.[29]

We calculated the energies (and corresponding reduction potentials) for all six localizations of the mixed-valence pair in the HiPIP II from *E. halophila*, again for various protein dielectric constants. The differences are 1−2 orders of magnitude smaller than in the case of Fe_2S_2 system. Although this may be partly due to the inadequacy of the treatment, we feel that it may also reflect a substantially more symmetric electrostatic environment around the polymetallic center in HiPIPs as opposed to Fe_2S_2 ferredoxins. The calculated values for a protein dielectric constant of 1 (to enhance the differences) are shown in Table 2. Even for this choice of dielectric constant, all different electronic distributions are within *kT*. It appears, however, that the calculated individual reduction potentials do provide the correct answer: the mixed-valence pair is preferably lying on the edge of the Fe_4S_4 cube which contains the Fe2 and Fe3 ions, as experimentally found.[59]

In the case of the high-potential ferredoxin from *C. vinosum*, it has been proposed that there are two isomers differing for the valence distribution as shown in Figure 3.[61] The experimental distribution is 60% Fe3−Fe4 over 40% Fe2−Fe3.[62] Since the reduced form contains four iron ions in the oxidation state 2.5+, we know that Fe3 bound to Cys 63 is the most reducible iron and Fe1 bound to Cys 77 is the least reducible iron, Fe2 and Fe4 having intermediate reduction potentials. In this case, the calculations show that the mixed-valence pairs Fe3−Fe4 and Fe2−Fe3 display the minimum energy, although the energy separations are small with respect to *kT*. The qualitative agreement for the calculated individual reduction potentials in both of these high-potential ferredoxins with the experimental results may be interpreted as a further indication that this type of calculation may be adequate to simulate microscopic effects. The differences in ΔE among the various electronic distributions in HiPIPs are, however, much smaller than that in Fe_2S_2 systems (cf. ΔE values in Tables 1 and 2, taking also into account that those in Table 2 are amplified by $\epsilon = 1$). It may be that a further contribution to the experimental ΔE values in Fe_4S_4 systems arises from the inequivalence of the cubane itself. Even in the most symmetric Fe_4S_4 center, the pair with mixed valence must have intermetal distances different from those in the ferric pair. In other words, if we add an electron to a hypothetical $Fe_4S_4^{4+}$ center containing four iron(III) ions, the electron delocalizes over two iron ions, giving rise to a mixed-valence pair. This changes the geometry of the center, presumably by increasing the iron−iron distance within the mixed-valence pair. In this view, the protein component might just trigger, through electrostatic interactions, a change in the structure that is then amplified by electronic effects. Of course, it is also possible that the steric constraints imposed by the protein induce a static distortion in the polymetallic center even if this is not observed experimentally in the X-ray structures. In both cases, quantomechanical contributions to the electrochemical properties would be operative which cannot be accounted for by an electrostatic model. In any event, this research has permitted a further step forward in the rationalization of fine electrostatic effects in proteins.

Concluding Remarks

The present calculations have confirmed that the net charges of acidic and basic groups account for the large variation in reduction potential within the series of high-potential ferredoxins. This result is essentially model-independent and is in contrast with any previous comparative analysis of the reduction potentials, particularly of cytochromes.[11] We found that this electrostatic contribution becomes significant in a series of small proteins with relatively large structural homology.

We then showed that the individual reduction potentials of the two iron ions in Fe_2S_2 proteins are correctly predicted and that solvation effects are those which mainly determine this feature of the reactivity of these proteins. In the case of Fe_4S_4 containing high-potential ferredoxins, the individual reduction potentials are only qualitatively reproduced. It is possible that the protein component induces geometric distortions that contribute to the differentiation among the individual irons and that cannot be taken into account with this kind of calculation.

(59) Banci, L.; Bertini, I.; Capozzi, F.; Carloni, P.; Ciurli, S.; Luchinat, C.; Piccioli, M. *J. Am. Chem. Soc.* **1993**, *115*, 3431−3440.
(60) Banci, L.; Bertini, I.; Ciurli, S.; Ferretti, S.; Luchinat, C.; Piccioli, M. *Biochemistry* **1993**, *32*, 9387−9397.
(61) Bertini, I.; Gaudemer, A.; Luchinat, C.; Piccioli, M. *Biochemistry* **1993**, *32*, 12887−12893.
(62) Bertini, I.; Capozzi, F.; Eltis, L. D.; Felli, I. C.; Luchinat, C.; Piccioli, M. *Inorg. Chem.* **1995**, *34*, 2516−2523.

In any case, the results suggest that the charge distribution within the polymetallic center in this class of proteins may be important in determining the electrostatical properties of the individual irons. It is interesting to note that the atomic charges proposed by Case for Fe_2S_2 and Fe_4S_4 clusters[22] can be successfully used to the present degree of refinement.

A final comment is due the value of the dielectric constant. If the electronic charges and polarizabilities were precisely known and the solvent effects treated properly, one would expect a dielectric constant of 2−4 to be appropriate. To describe the properties within the series of high-potential ferredoxins, a larger effective value is needed. In the case of the individual potentials, it is possible that the short-range electrostatic effects between the iron ions, and the partial charges around each, require a value closer to 1. For Fe_2S_2 proteins, the results of the calculations are consistent with the experimental results and are independent of the choice of dielectric constant in the 1−15 range.

IC960051Q